

# Fracture modes in alumina at hypervelocity impact conditions

I. GILATH, S. ELIEZER, Y. GAZIT  
Soreq Nuclear Research Center, Yavne 70600, Israel

Experiments were performed to find the fracture patterns of alumina at hypervelocity impact conditions using short pulsed laser induced shock waves. For planar shock waves spalling was obtained, while using spherical shock waves, the samples developed Herzian (conical) fracture mode.

## 1. Introduction

The dynamic behaviour of high strength ceramics is of interest because of the expanding use of these materials in high pressure, shock wave technologies and in military applications as components of armour systems. Ceramics are brittle materials and fracture occurs by brittle crack propagation up to shattering. A glassy phase is added (few percentage) to the alumina [1] to ease the preparation. This second phase is degrading the dynamic properties because of the impedance mismatch at the phase boundaries during shock wave propagation. The dynamic properties such as spall strength, Hugoniot elastic limit and Equation of State of alumina have been studied using explosive [2] or gas gun plate impact experiments [3–5].

Short pulsed laser is a convenient experimental method to apply intense stress pulses for very short time. The shock wave pressure,  $P$ , is related to laser pulse intensity,  $I$ , scaling approximately as  $P \approx I^{3/4}$  in a manner almost independent of the material. A  $1.3 \times 10^5$  MPa pressure is obtained on the ablation surface of an aluminium slab for an irradiation level of  $I = 10^{13}$  W cm<sup>-2</sup>. This short time high pressure enables one to study the dynamic fracture modes of materials at ultra high strain rate [6–10] of about  $10^7$  s<sup>-1</sup>. The laser beam can be delivered to the target in one dimensional stress conditions [9] corresponding to plate impact or spherical shock wave conditions corresponding to projectile impact. When beam diameter is at least three times greater than target thickness, than one dimensional conditions prevail, while with focused beam, spherical shock waves can be obtained. Different failure patterns are expected to occur when using the above impact geometries for strong brittle solids as ceramics.

In this work, experiments were performed to find the fracture patterns of alumina at hypervelocity impact conditions using short pulsed laser induced shock waves.

## 2. Experimental procedure

A high-irradiance single-beam pulsed Nd:glass laser [6–10] was used to generate the shock waves in

alumina targets. The modified Gaussian laser pulse had a 3 ns full width at half maximum intensity and 1.1 ns rise and decay times. The successive amplifier stages deliver up to 80 J energy corresponding to  $10^{11}$ – $10^{13}$  W cm<sup>-2</sup> and can be controlled for stepwise energy changes for damage evolution monitoring. The laser spot diameter can be changed from 0.15–3 mm. The focused beam (0.15 mm diameter) was used for spherical shock waves while the large diameter spots were used for one dimensional shock wave conditions. Alumina ceramic targets were prepared by diamond cutting and polishing slices from a AD-90 tile [1]. Target thicknesses ranged between 0.25–4 mm. Damage was evaluated using scanning electron microscopy (SEM) and dye impregnation for crack pattern enhancement on sectioned samples.

## 3. Results

For planar shock wave conditions, spall damage was observed on the back (free) surface of the impacted target in the form of a shallow plane circular crater, see Fig. 1. Spall damage is a fracture resulting from tensile stresses developed in the material due to reflected shock waves and rarefaction waves. Similar spall craters were observed in metals [6–10]. The energy density for spall layer detachment was found  $500 \pm 50$  J cm<sup>-2</sup> for alumina as compared to iron  $5300 \pm 50$  J cm<sup>-2</sup> for similar experimental conditions [6].

On the front surface (laser side) no crater was observed but some increase in porosity, see Fig. 2. In Fig. 3, an enlarged detail from Fig. 2 can be seen revealing surface sintering of ceramics as a result of laser induced surface melting, with many micron and submicron size circular voids. The microcracks and voids resulted from rapid cooling following the melting. In Fig. 4 a detail is shown of the back surface fracture (spall crater) where intergranular and transgranular fracture can be observed. The angle of divergence measured for damage extension was  $58 \pm 3^\circ$ . The angle was calculated from the impact damage diameter on the front compared to damage diameter on the back for a definite sample thickness. No radial

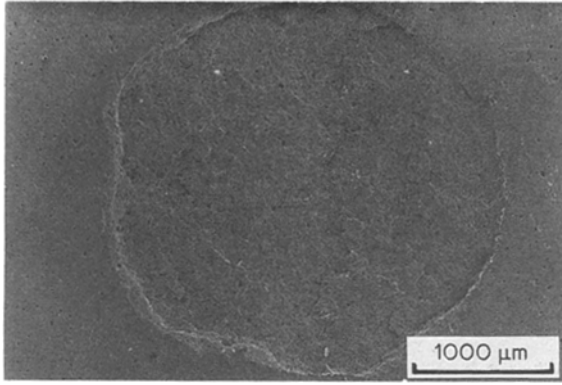


Figure 1 Back surface spall of ceramics impacted in plane shock wave conditions.

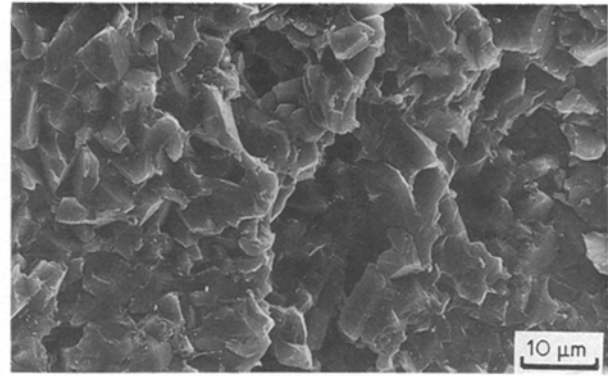


Figure 4 Detail from Fig. 1 showing mixed mode fracture.

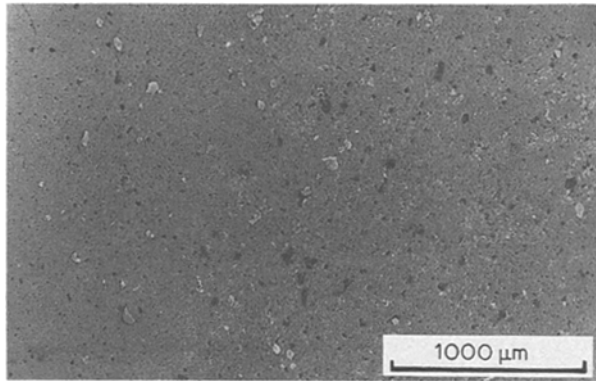


Figure 2 Front surface damage of ceramics impacted in plane shock wave conditions.

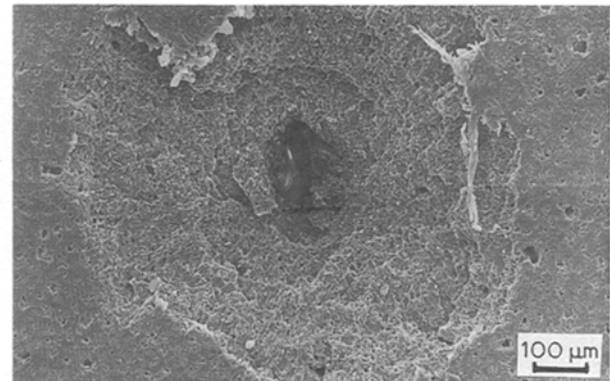


Figure 5 Cone cracking in ceramics for spherical shockwave conditions.

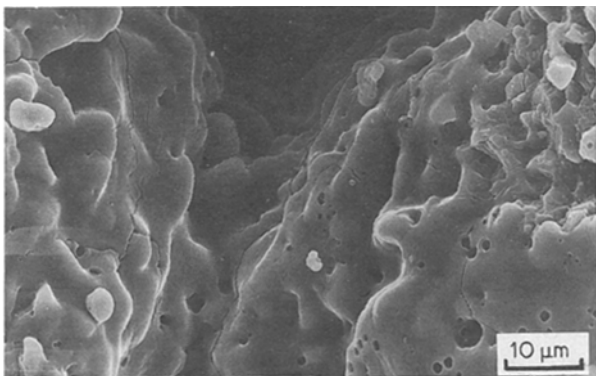


Figure 3 Detail from Fig. 2 showing surface melting.

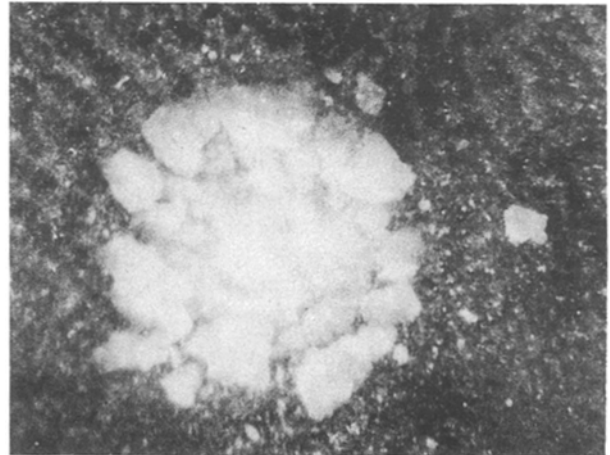


Figure 6 Collected debris from cone cracking (50 ×).

cracks have been observed on any of the impacted samples below  $2000 \text{ J cm}^{-2}$ . Above this value, the samples were shattered by radial cracking and spalling.

For spherical shockwave conditions, cone cracking was observed in ceramics. The development of Herzian cone cracks was studied in glass, being an isotropic transparent brittle solid, but can be applied to a wide variety of other strong brittle materials [11, 12]. Cone crack fracture mode was observed in all samples where laser spot size was smaller than target thickness, see Fig. 5. We used a laser spot size of 0.15 mm and samples of 0.25, 0.36, 1 and 4 mm thickness. The expelled cone was recovered in the form of fragments of varying sizes (0.01–0.15 mm) see Fig. 6.

The angle of divergence measured for damage extension was  $74 \pm 5^\circ$ .

In Fig. 7 the shock wave damage pattern in ceramics is revealed on a sectioned sample. The damage pattern is visible due to dye impregnation. The energy density was  $100 \pm 2 \text{ kJ cm}^{-2}$  for a 1 mm thick sample. The damage extent was about half way through the sample thickness. The angle of damage dispersion was only  $40^\circ$  for the highest energy density. This finding is interpreted as the damage dispersion angle decreases with increasing shock wave velocity for hypervelocity impact conditions.

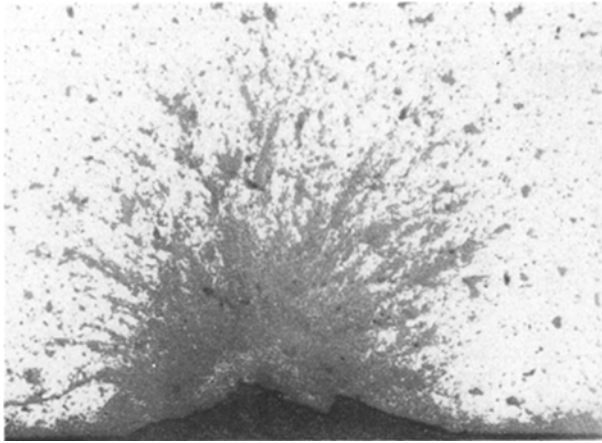


Figure 7 Shock wave damage pattern as revealed by dye absorption on a sectioned alumina sample ( $100\times$ ).

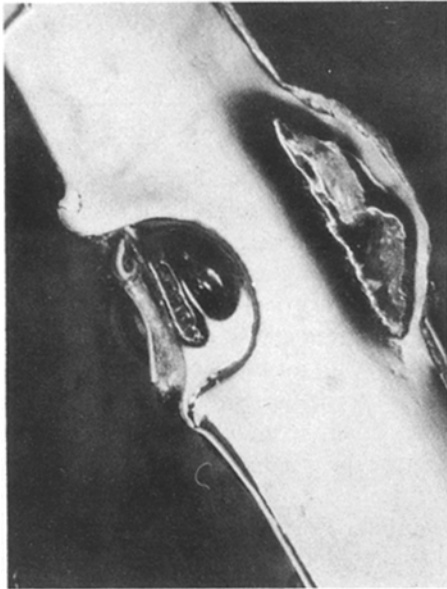


Figure 8 Damage in aluminium for spherical shock waves ( $35\times$ ).

In Fig. 8, a cross section of an impacted aluminium sample is presented. The impact conditions and sample thickness are identical as above. In aluminium a hemispherical crater is formed on the front (laser

side) as compared to the very shallow crater for the ceramics as can be seen in Fig. 7. The spall layer extension (back) in aluminium is just slightly larger than the damage on the front.

In summary, evidence has been presented confirming the different fracture patterns in ceramics for plane and spherical shock waves for hypervelocity impact conditions.

### Acknowledgements

The authors wish to thank Y. Sapir and S. Maman for their able technical assistance.

### References

1. COORS PORCELAIN COMPANY CERAMICS, in "Materials for tough jobs", Bulletin No. 953.
2. D. E. MUNSON and R. J. LAWRENCE, *J. Appl. Phys.* **50** (1979) 6272.
3. D. YAZIV, S. J. BLESS and Z. ROSENBERG, *ibid.* **58** (1985) 3415.
4. J. CAGNOUX and F. LONGY, *J. de Physique* **49** (1988) 3.
5. Y. YESHURUN, D. G. BRANDON, A. VENKERT and Z. ROSENBERG, *ibid.* **49** (1988) 11.
6. I. GILATH, S. ELIEZER, M. P. DARIEL and L. KORNBLITH, *J. Mater. Sci. Lett.* **7** (1988) 915.
7. I. GILATH, D. SALZMAN, M. GIVON, M. P. DARIEL, L. KORNBLITH and T. BAR NOY, *J. Mater. Sci.* **23** (1988) 1825.
8. I. GILATH, S. ELIEZER, M. P. DARIEL and L. KORNBLITH, *Appl. Phys. Lett.* **52** (1988) 1207.
9. D. SALZMANN, I. GILATH and B. ARAD, *ibid.* **52** (1988) 1128.
10. I. GILATH, S. ELIEZER, M. P. DARIEL, L. KORNBLITH and T. BAR NOY, *J. de Physique* **49** (1988) 191.
11. T. R. WILSHAW, *J. Phys. D. Appl. Phys.* **4** (1971) 1567.
12. H. P. KIRCHNER and R. M. GRUVER, *J. Mater. Sci.* **28** (1977) 153.

Received 14 July  
and accepted 17 October 1989